Supporting Information

Linking Defects, Hierarchical Porosity Generation and Desalination Performance in Metal-Organic Frameworks

Weibin Liang[#], Lin Li[#], Jingwei Hou[*], Nicholas D. Shepherd, Thomas D. Bennett, Deanna M. D'Alessandro[*], Vicki Chen

Dr. W. Liang, N. D. Shepherd, A. Prof. D.M. D'Alessandro

School of Chemistry, The University of Sydney, NSW 2006, Australia.

L. Li, Dr. J. Hou, Prof. V. Chen

UNESCO Center for Membrane Science and Technology, School of Chemical Engineering,

The University of New South Wales, NSW 2052, Australia.

Dr. J. Hou, Dr. T. D. Bennett

Department of Materials Science and Metallurgy, University of Cambridge, Cambridge CB3

0FS, UK.

[#]These authors contributed equally to this work.

Contents

S1 Materials

All chemicals and solvents for MOF synthesis were purchased from commercial sources and used as received without further purification.

Commercial hydrophilic PVDF hollow fibre membranes (outer diameter: 1.2 mm, thickness: 275 μm, average pore size: 0.04 μm, provided by MEMCOR®-Evoqua) were used in this study as substrate. Polyvinyl alcohol (PVA, Mw 89k-98k, 99+% hydrolysed) and humic acid sodium salt were purchased from Sigma-Aldrich. All other chemicals were of the highest purity and used without further purification.

S2 MOF syntheses - microwave-assisted MIL-53(Al) syntheses

Table S1. Synthesis conditions for the MIL-53(Al) samples.

Entry[a]	$Al_2(SO_4)_3.18H_2O$		Fumaric acid		Urea		H_2O [mL]	T [°C][b]	Time [min]
	[mg]	[mmol]	[mg]	[mmol]	[mg]	[mmol]			
$1_{0.25}$	128	0.19	45	0.39	276	4.6	20	130	30
$1_{0.5}$	256	0.38	90	0.78	276	4.6	20	130	30
1_{1}	256	0.38	90	0.78	276	4.6	10	130	30
1_{2}	512	0.77	180	1.55	276	4.6	10	130	30
1_{4}	1024	1.54	360	3.10	276	4.6	10	130	30
$1_{1,15min}$	256	0.38	90	0.78	276	4.6	10	130	15
$1_{1,45min}$	256	0.38	90	0.78	276	4.6	10	130	45
$1_{1,60min}$	256	0.38	90	0.78	276	4.6	10	130	60

[a]1 = MIL-53(Al); [b]Temperature ramp to 130 °C within 1 min.

S3 X-ray powder diffraction (XRPD) and Le Bail cell simulation

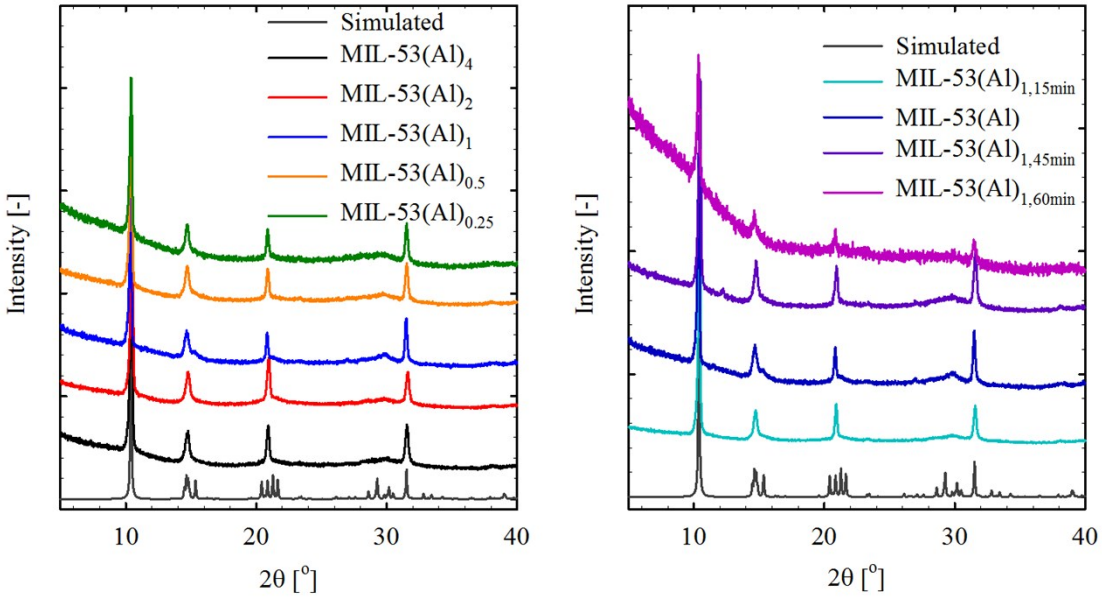

Figure S1. XRPD patterns for activated MIL-53(Al) samples.

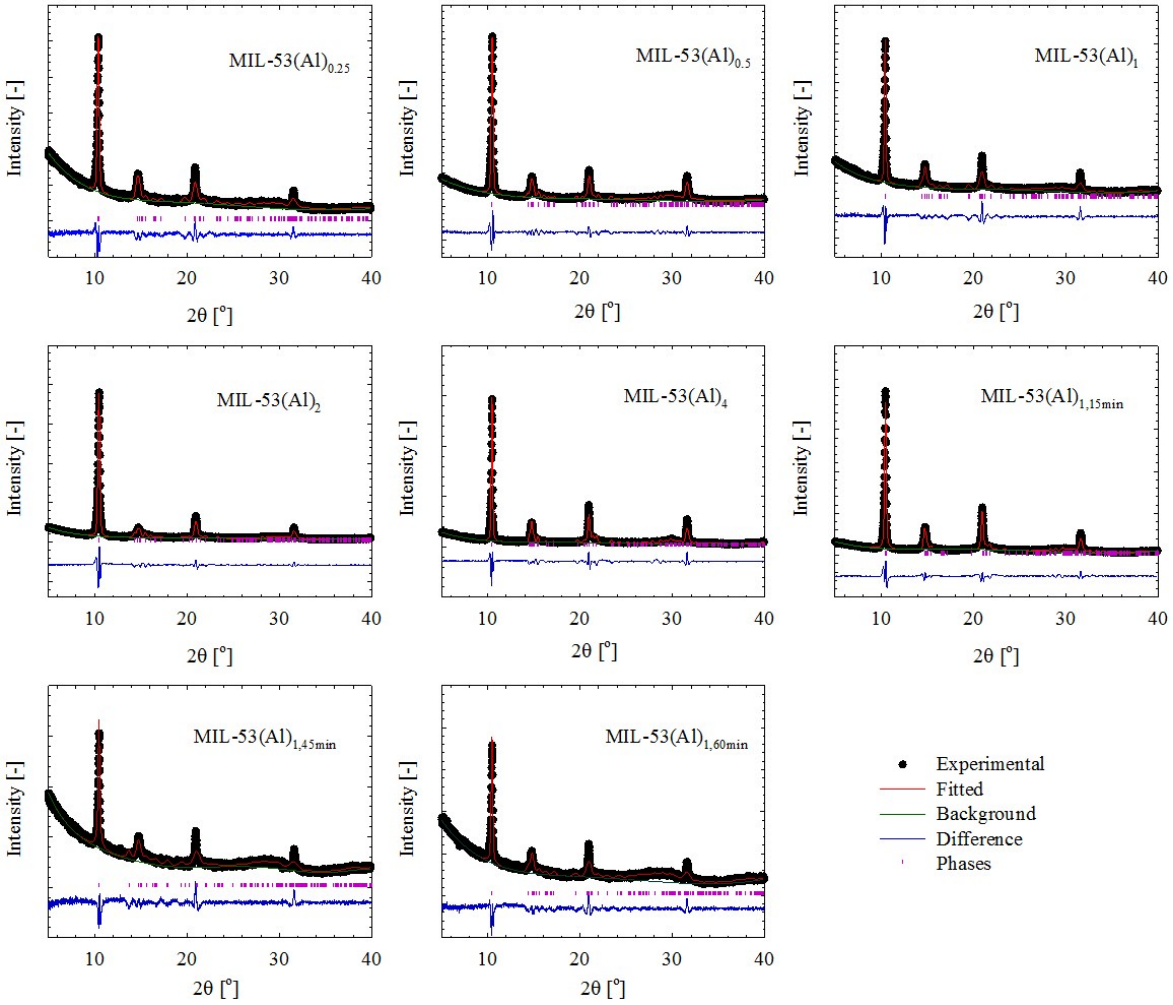

Figure S2. *Le Bail* refinements of MIL-53(Al) samples show the experimental (black), fitted (red), and difference (blue) patterns. The positions of the Bragg peaks are indicated by the pink bars.

Table S2. Simulated *Le Bail* cell parameters for MIL-53(Al).

Entry[a]	Space group	Cell parameter						Volume [Å^3]	R_{wp} [%]
		α [°]	β [°]	γ [°]	a [Å]	b [Å]	c [Å]		
$1_{0.25}$	$P2_1/c$	90	121.58(1)	90	6.69(1)	12.11(1)	13.98(1)	965.59(5)	7.96
$1_{0.5}$	$P2_1/c$	90	123.80(1)	90	6.88(1)	12.05(1)	14.31(1)	985.96(3)	8.68
1_1	$P2_1/c$	90	122.45(1)	90	6.77(1)	12.32(1)	13.85(1)	975.04(3)	7.52
1_2	$P2_1/c$	90	123.89(1)	90	6.87(1)	12.07(1)	14.30(1)	985.10(4)	8.92
1_4	$P2_1/c$	90	122.58(1)	90	6.83(1)	12.01(1)	14.19(1)	980.47(3)	10.80
$1_{1,15min}$	$P2_1/c$	90	121.36(1)	90	6.73(1)	12.06(1)	13.83(1)	959.18(2)	10.76
$1_{1,45min}$	$P2_1/c$	90	127.86(1)	90	6.90(1)	12.00(1)	15.00(1)	979.64(8)	7.78
$1_{1,60min}$	$P2_1/c$	90	122.37(1)	90	6.75(1)	12.32(1)	13.80(1)	969.65(5)	8.03

[a]1 = MIL-53(Al).

S4 Potentiometric acid-base titration

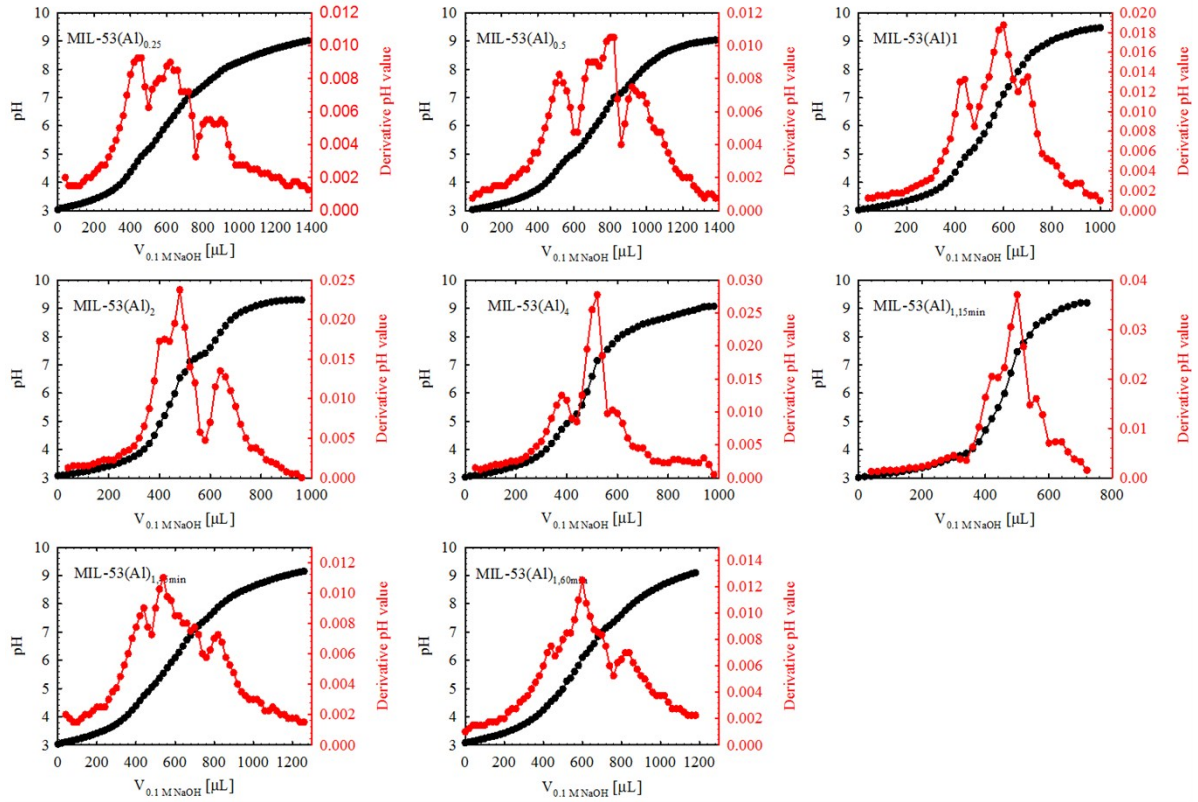

Figure S3. Potentiometric acid-base titration curves for MIL-53(Al) frameworks.

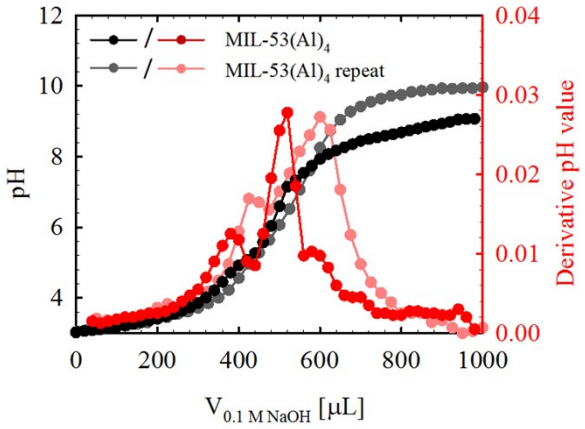

Entry	pK_{a1}	pK_{a2}	pK_{a3}
MIL-53(Al)$_4$	3.39	3.63	-
MIL-53(Al)$_4$ repeat	3.43	3.69	-

Figure S4. Potentiometric acid-base titration curves for MIL-53(Al)$_4$.

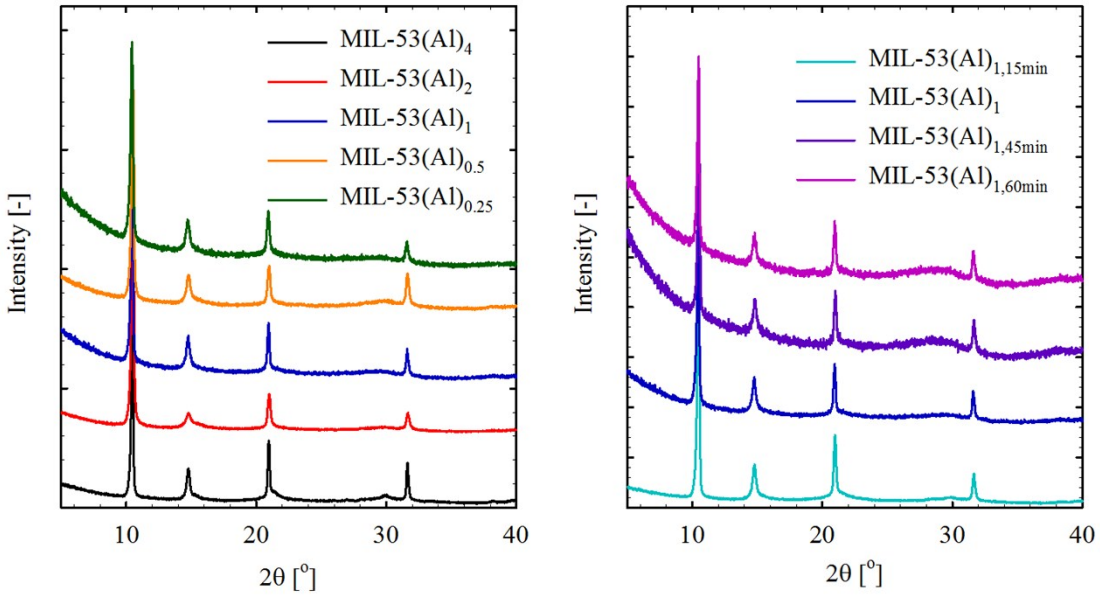

Figure S5. XRPD patterns for MIL-53(Al) samples after potentiometric acid-base titration.

S5 Scanning electron microscopy (SEM)

Field-emission SEM (FE-SEM) images were obtained using a Zeiss ULTRA plus microscope (working distance ~9 mm; acceleration voltage 20 kV). Samples were prepared by dispersing the powdered solids in ethanol to produce a suspension that was deposited onto a carbon block and dried in air.

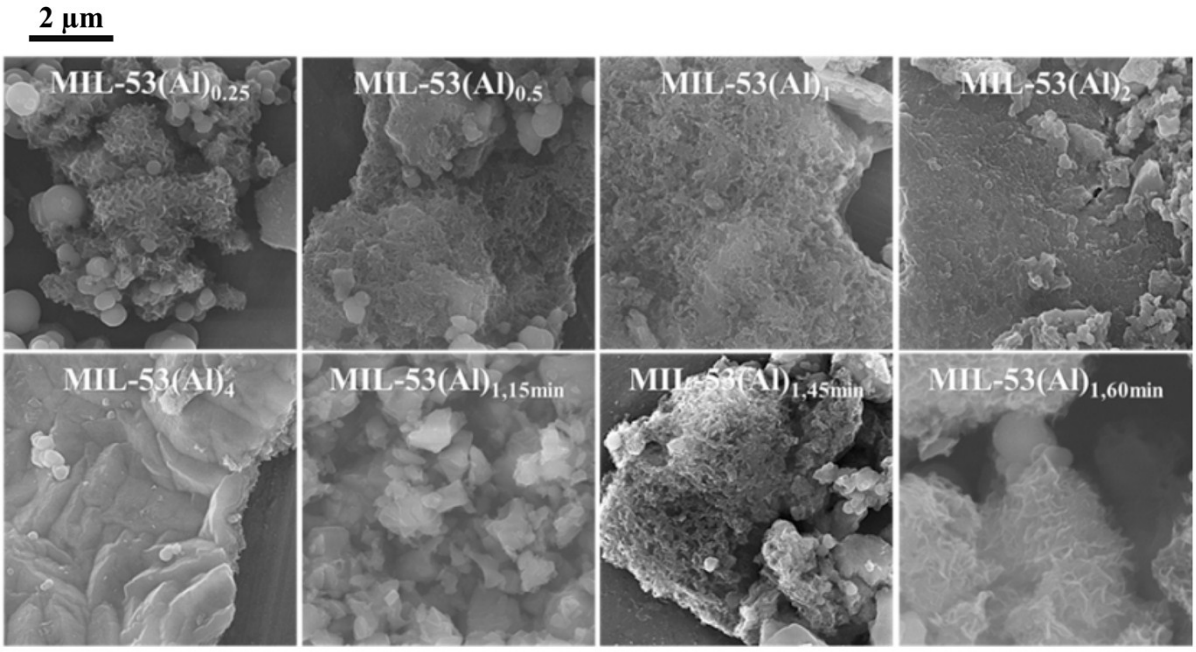

Figure S6. SEM images for MIL-53(Al) samples at a magnification level of 10 K.

S6 77 K N_2 sorption analysis

N_2 sorption isotherms were recorded on a 3Flex Surface Characterisation Analyser (Micromeritics Instruments Inc.). Approximately 100 mg of the powdered solid was loaded into a glass analysis tube and outgassed for 16 h under dynamic vacuum (~10^{-6} bar) at 80 °C. N_2 adsorption and desorption isotherms were measured at 77 K and the surface areas were calculated using the Brunauer-Emmett-Teller (BET) model.[1]

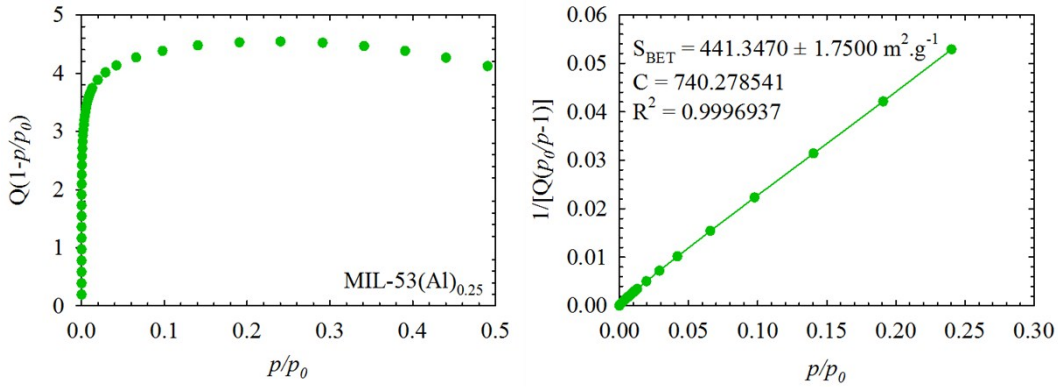

Figure S7. Consistency plot (left) and BET fit for MIL-53(Al)$_{0.25}$.

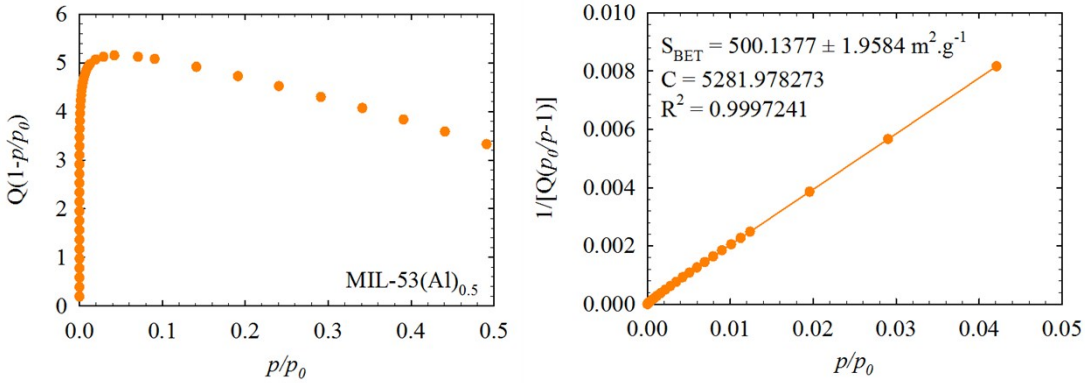

Figure S8. Consistency plot (left) and BET fit for MIL-53(Al)$_{0.5}$.

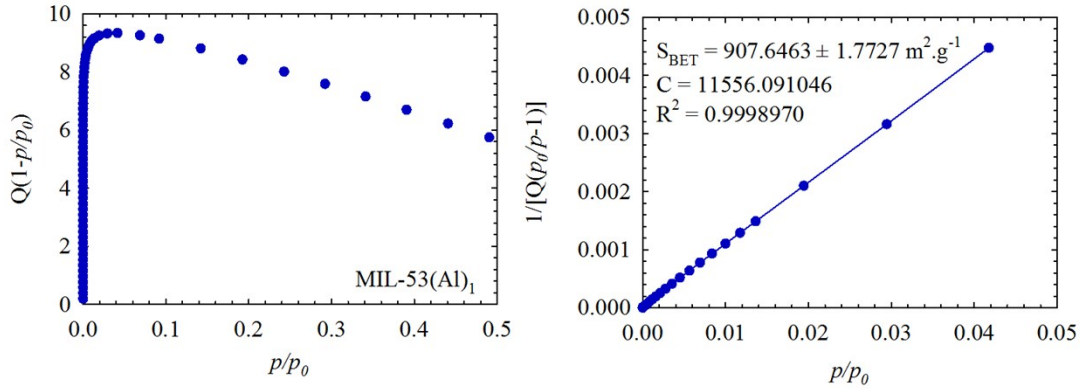

Figure S9. Consistency plot (left) and BET fit for MIL-53(Al)$_{1}$.

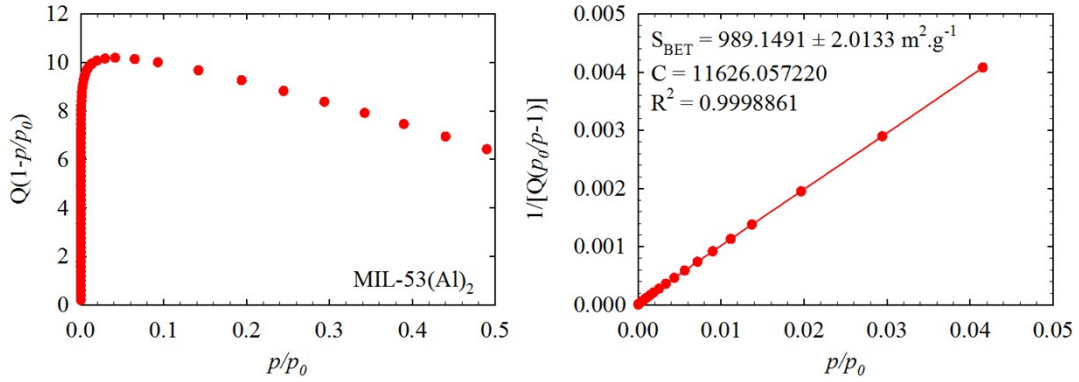

Figure S10. Consistency plot (left) and BET fit for MIL-53(Al)$_2$.

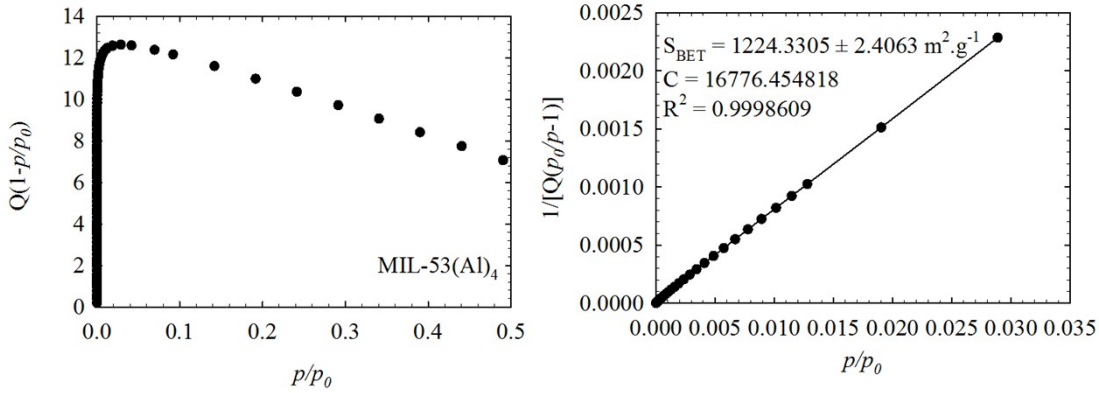

Figure S11. Consistency plot (left) and BET fit for MIL-53(Al)$_4$.

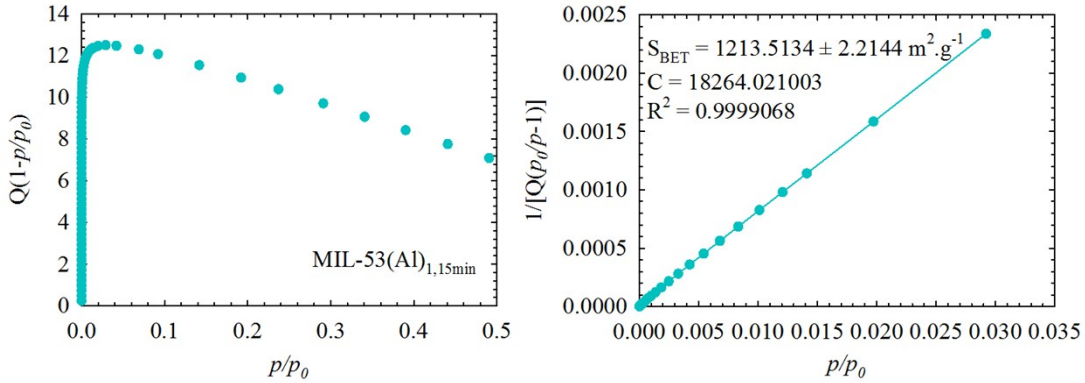

Figure S12. Consistency plot (left) and BET fit for MIL-53(Al)$_{1,15min}$.

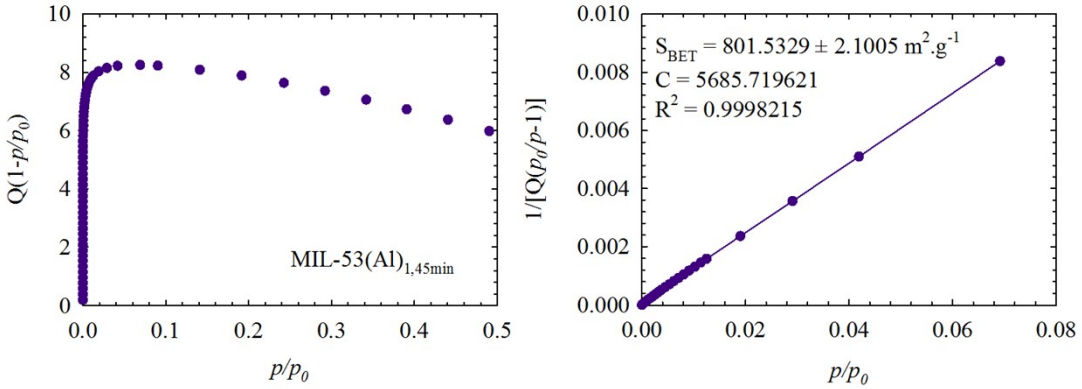

Figure S13. Consistency plot (left) and BET fit for MIL-53(Al)$_{1,45min}$.

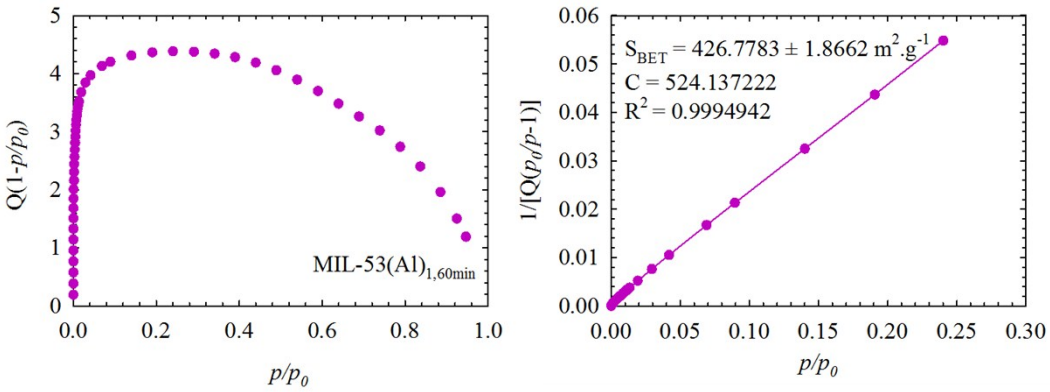

Figure S14. Consistency plot (left) and BET fit for MIL-53(Al)$_{1,60min}$.

The pore size distribution calculations were carried out using the DFT package (non-local density functional theory calculations, NLDFT, based on the N_2-Cylindrical Pores – Oxide Surface DFT model)[2] or Barrett-Joyner-Halenda (BJH) model[3] in the MicroActive software (version 3.00, Micromeritics Instuments Inc.).

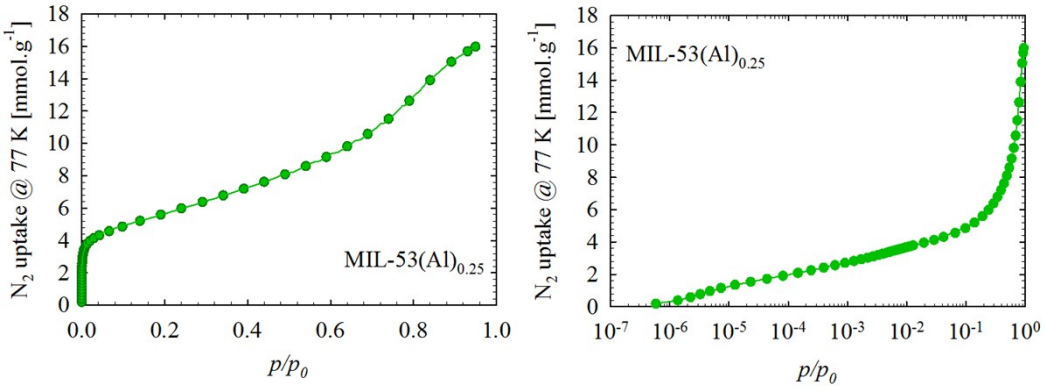

Figure S15. Goodness of fit (left) and log goodness (right) of fit plots of N_2 adsorption isotherm for MIL-53(Al)$_{0.25}$.

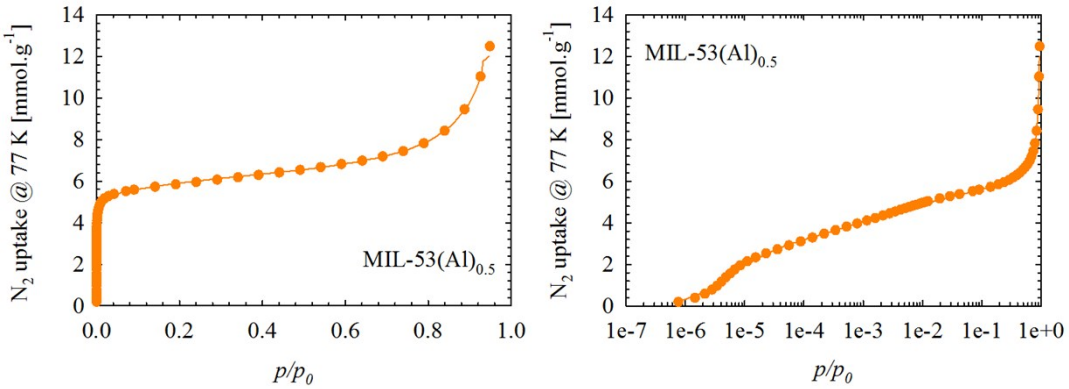

Figure S16. Goodness of fit (left) and log goodness (right) of fit plots of N_2 adsorption isotherm for MIL-53(Al)$_{0.5}$.

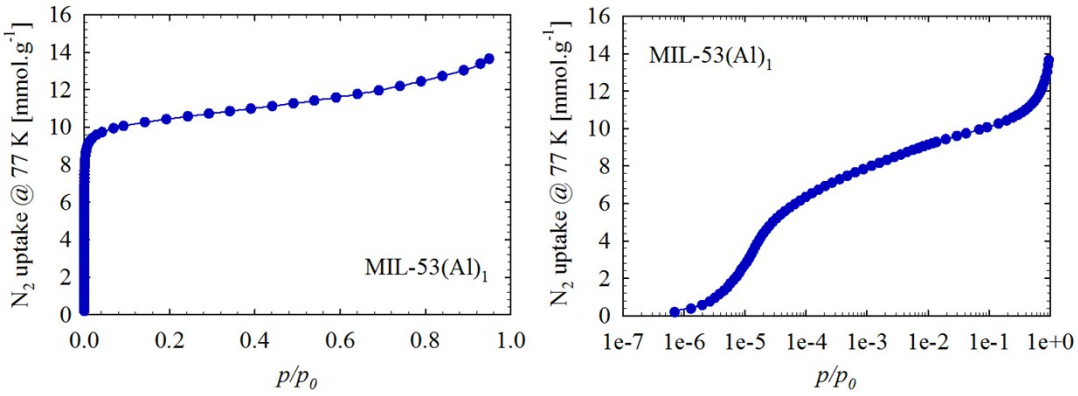

Figure S17. Goodness of fit (left) and log goodness (right) of fit plots of N_2 adsorption isotherm for MIL-53(Al)$_1$.

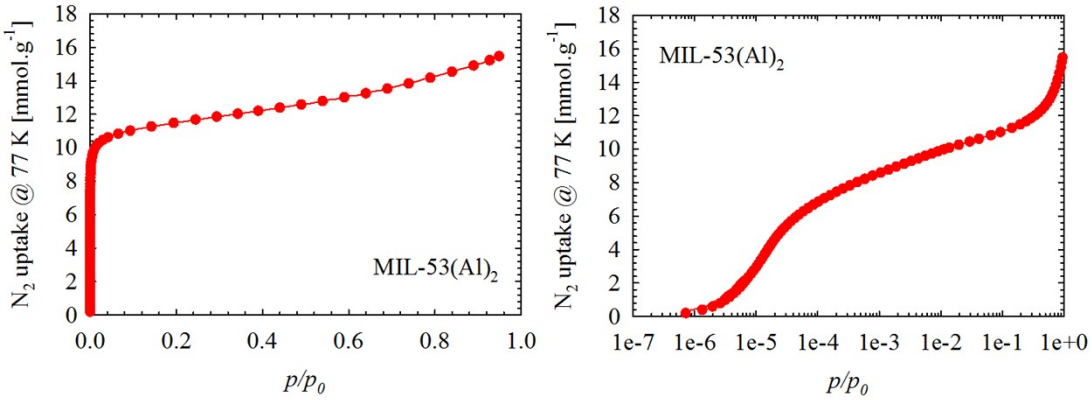

Figure S18. Goodness of fit (left) and log goodness (right) of fit plots of N_2 adsorption isotherm for MIL-53(Al)$_2$.

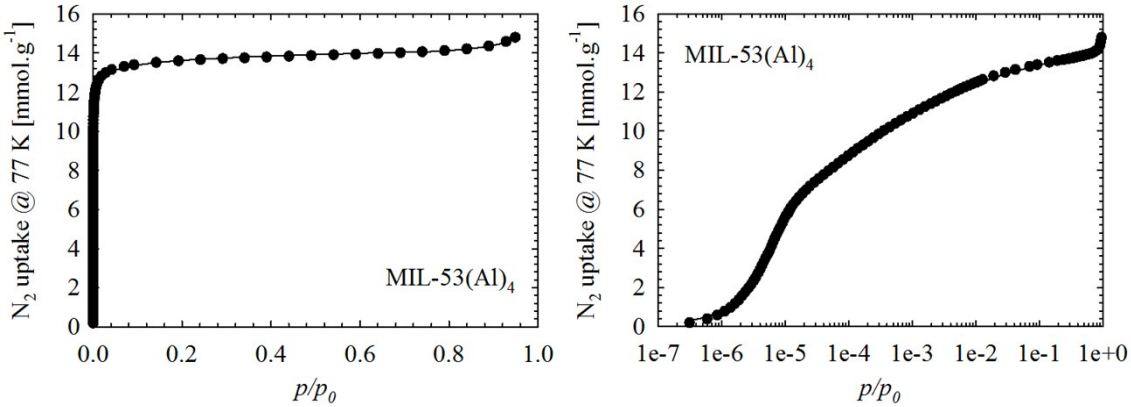

Figure S19. Goodness of fit (left) and log goodness (right) of fit plots of N_2 adsorption isotherm for MIL-53(Al)$_4$.

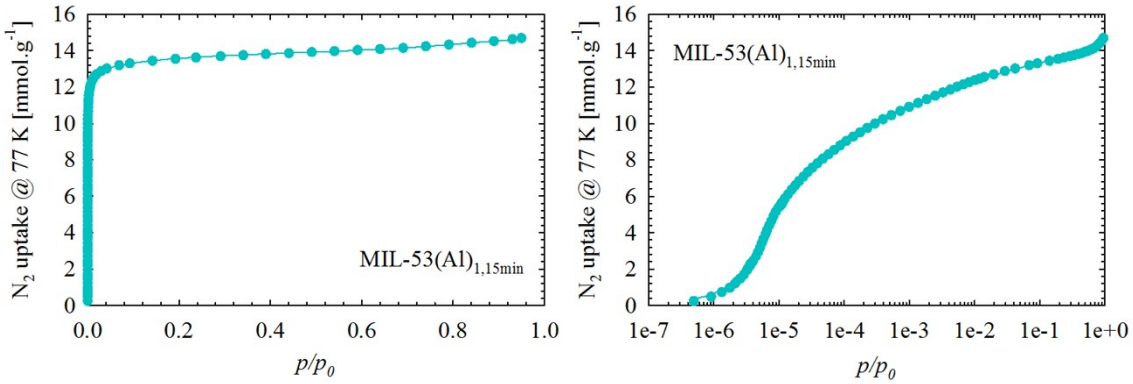

Figure S20. Goodness of fit (left) and log goodness (right) of fit plots of N_2 adsorption isotherm for MIL-53(Al)$_{1,15min}$.

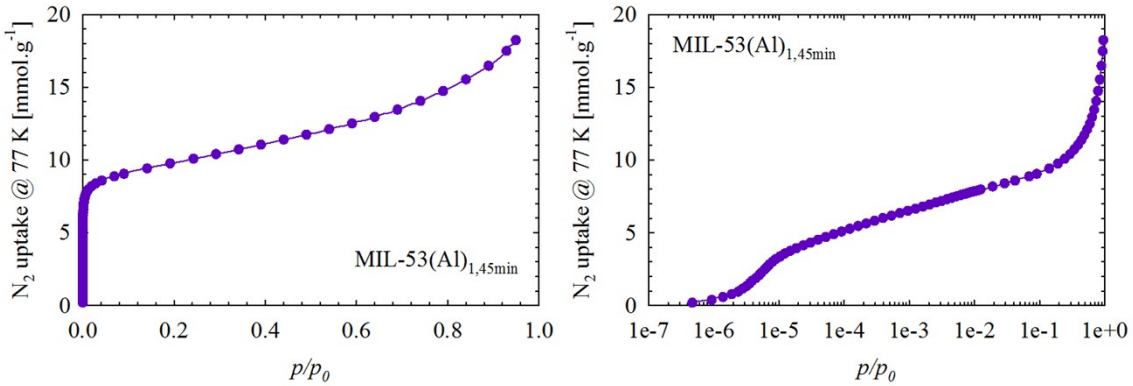

Figure S21. Goodness of fit (left) and log goodness (right) of fit plots of N_2 adsorption isotherm for MIL-53(Al)$_{1,45min}$.

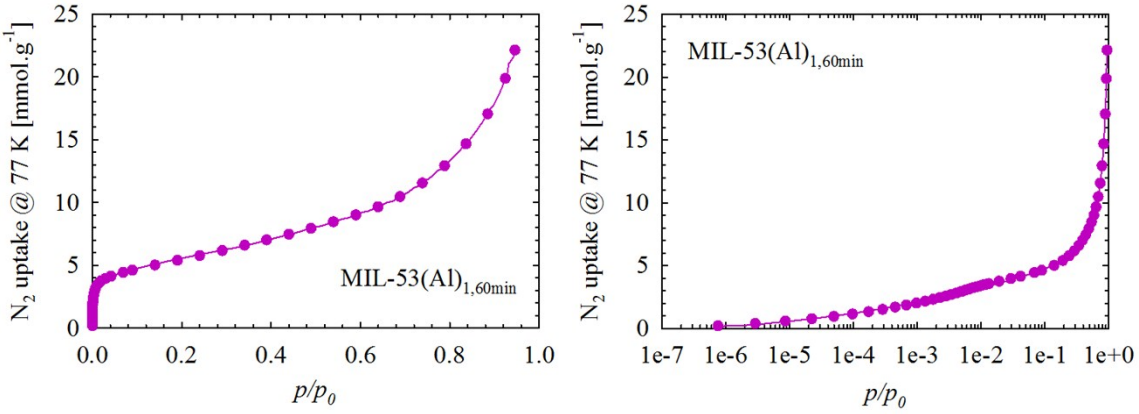

Figure S22. Goodness of fit (left) and log goodness (right) of fit plots of N_2 adsorption isotherm for MIL-53(Al)$_{1,60min}$.

S7 SEM and EDX analysis of the nanocomposite membranes

Surface and cross-section of the membranes were characterized by field emission scanning electron microscopy (FE-SEM, FEI Nova NanoSEM). Membrane cross-sectional samples were prepared by snapping in liquid nitrogen. All samples were sputter coated with platinum prior to imaging. The membrane surface component was analysed by energy dispersive X-ray spectroscopy (EDX, FEI Nova NanoSEM and Hitachi S3400).

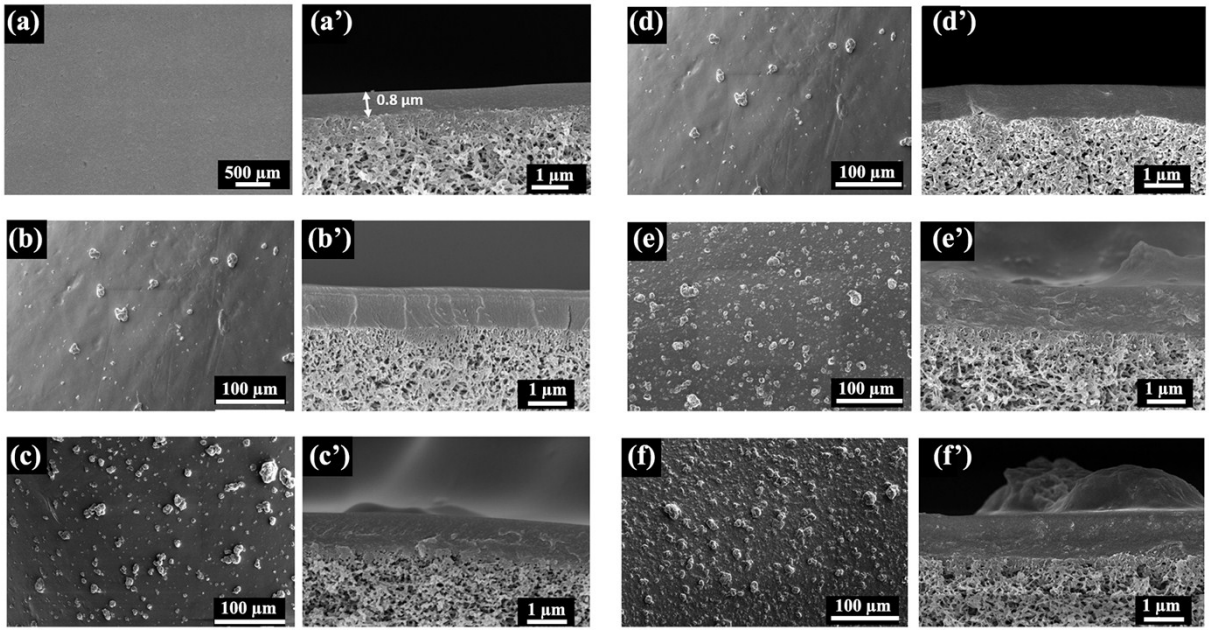

Figure S23. Surface and cross-sectional SEM image of composite membrane samples on PVDF supports: a) PVA; b) 10 % MIL-53(Al)$_{1,15min}$/PVA; c) 30 % MIL-53(Al)$_{1,15min}$/PVA; d) 10 % MIL-53(Al)$_{1,60min}$/PVA; e) 30 % MIL-53(Al)$_{1,60min}$/PVA; and f) 40 % MIL-53(Al)$_{1,60min}$/PVA.

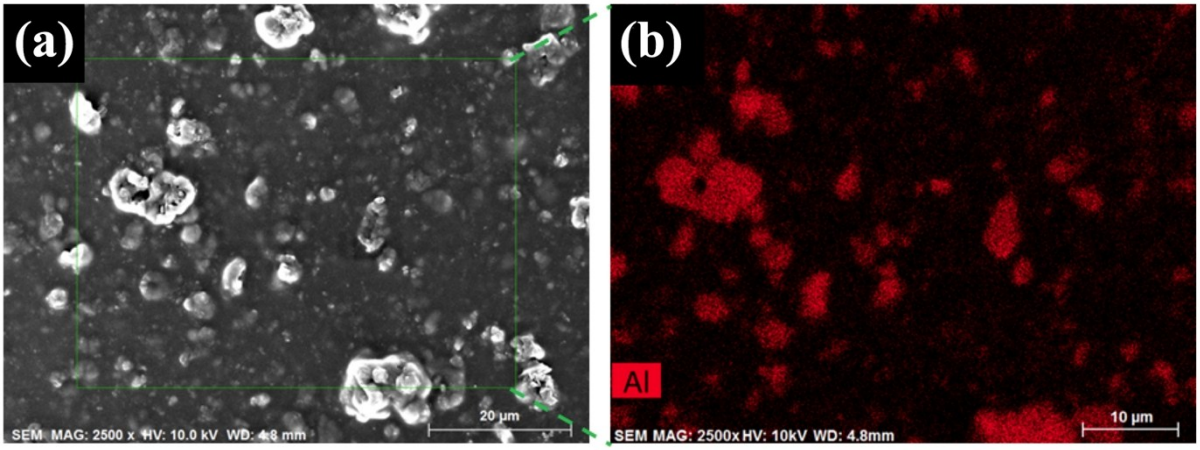

Figure S24. Surface EDX image and its reference SEM image for composite membrane with 30 % MIL-53(Al)$_{1,60min}$/PVA.

S8 Mechanical tensile strength test for the nanocomposite membranes

The tensile strength of the hollow fibre membranes was tested with the textural analyzer (TAXT2, Stable Micro Systems). The sample length was 100 mm, and the testing speed was 0.5 mm/s. The change of the stress under different elongation rate was recorded. At least 6 samples were tested and the average value was reported here.

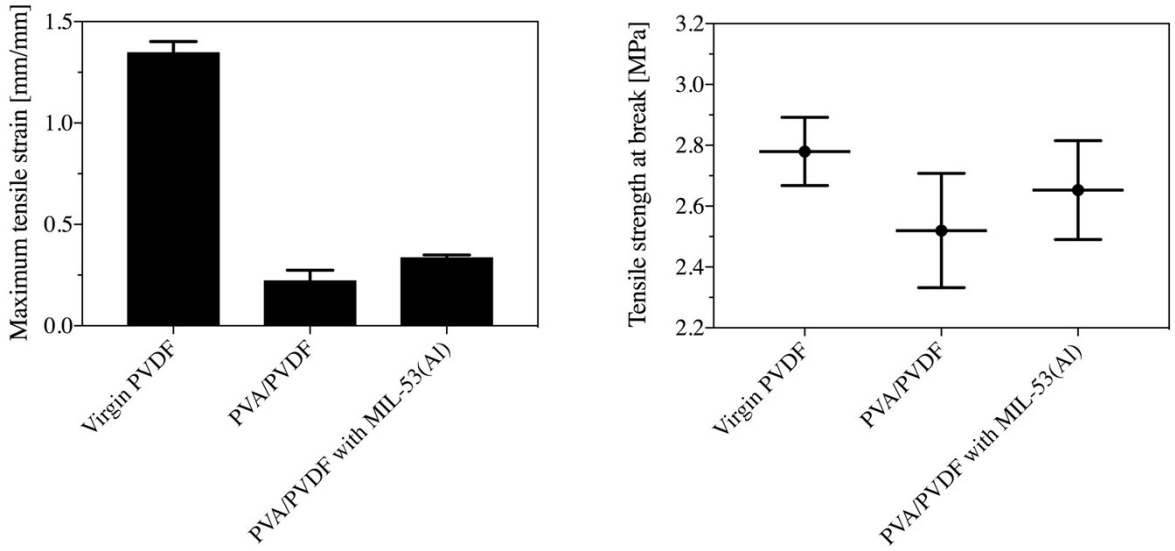

Figure S25. Tensile strength of the nanocomposite membranes. The composite hollow fiber membrane samples contained 30 wt % $MIL(53)_{1,60min}$.

S9 Water uptake by the MIL-53(Al)/PVA composites (FT-IR and film water uptake)

FT-IR (Spotlight 400, PerkinElmer) was used to characterize the surface properties of composite membranes. Water uptake for the film is measured to assess the membranes swelling ability, as the ratio of the weight of water in the film to the weight of the dry film at equilibrium hydration.

$$Uptake = \frac{m_W - m_d}{m_d} \times 100\% \qquad \text{(Equation S1)}$$

Where m_w and m_d represent the weight of cross-linked PVA at equilibrium hydration and dry state.

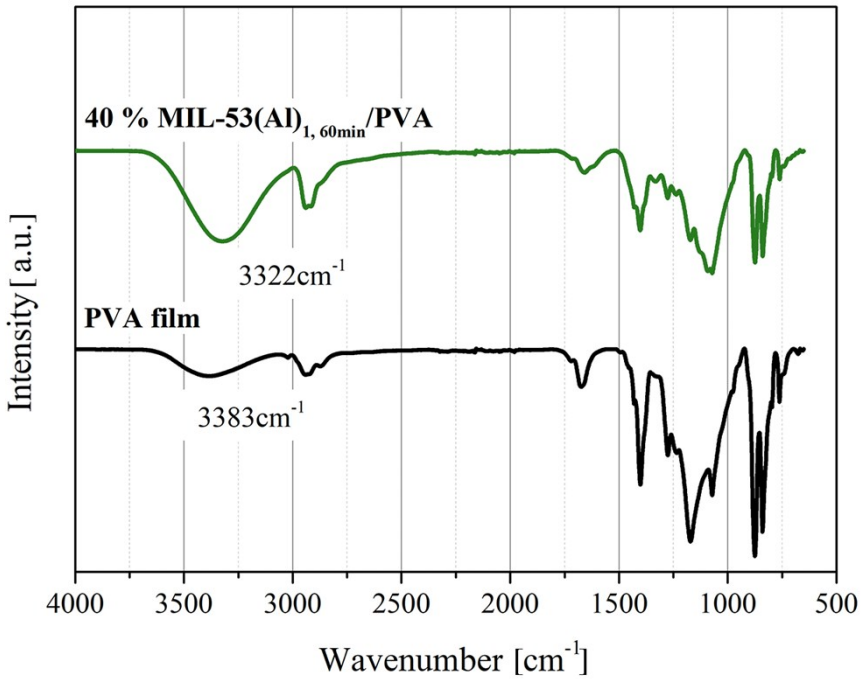

Figure S26. FT-IR spectrum for PVA and MIL-53(Al)/PVA films.

Table S3 Water uptake value for freestanding PVA films with different MIL-53(Al)

Film sample	Uptake (%)
Pure PVA	29.6±0.3
MIL-53(Al)-15min, 10 wt. %	29.6±0.7
MIL-53(Al)-15min, 30 wt. %	33.5±1.4
MIL-53(Al)-60min, 10 wt. %	38.6±1.5
MIL-53(Al)-60min, 30 wt. %	39.1±0.5
MIL-53(Al)-60min, 40 wt. %	32.7±1.0

S10 Thermal analysis of the PVA freestanding films

Thermal analysis was conducted using a Differential scanning calorimetry (DSC Q20, TA Instruments, Inc., USA). The samples are heated from -30 °C to 300 °C at a rate of 10 °C/min in a nitrogen atmosphere. Thermal gravimetric analysis (TGA) measurement was carried out by using a TGA Q5000 (TA instruments, Inc., USA) in nitrogen atmosphere. The sample was heated from Room temp to 800°C at a rate of 10°C/min.

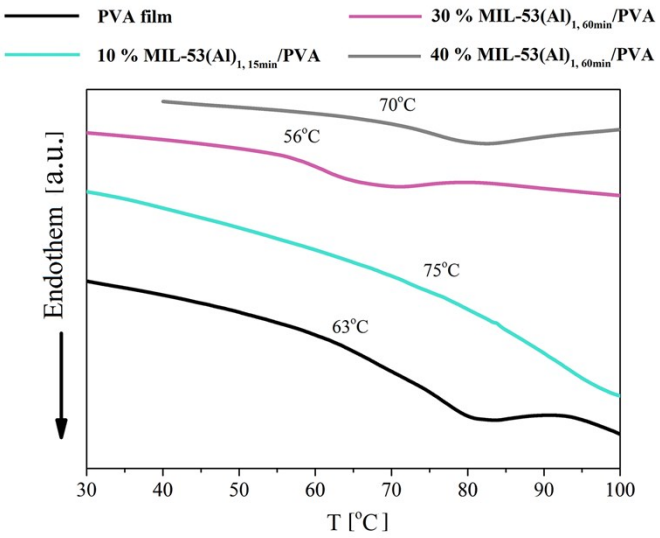

Figure S27. Differential scanning calorimetry of PVA and MIL-53(Al)/PVA mixed matrix films.

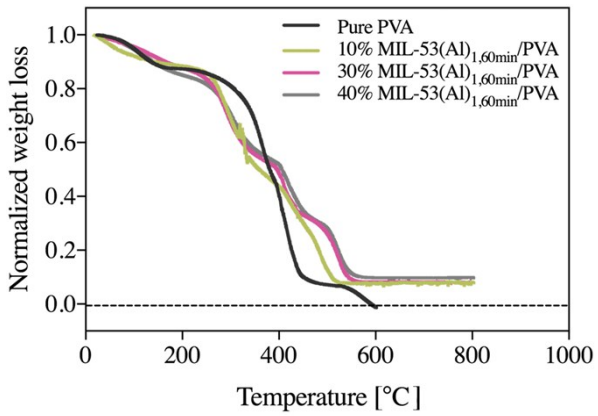

Figure S28. Thermogravimetric analysis (TGA) results of the MIL-53(Al)/PVA films.

S11 Crystallinity characterization of MIL-53(Al)/PVA films

Crystallinity analysis was carried out with XRD instrucment (PANalytical Empyrean X-ray diffraction system, Cobalt) with Cu K_α radiation. For PVA, the board peak at around 19 degree aligns its amorphous nature. For the mixed matrix films, the distinct XRD peaks for MIL-53(Al) was only observed when the filling loading was relatively high.

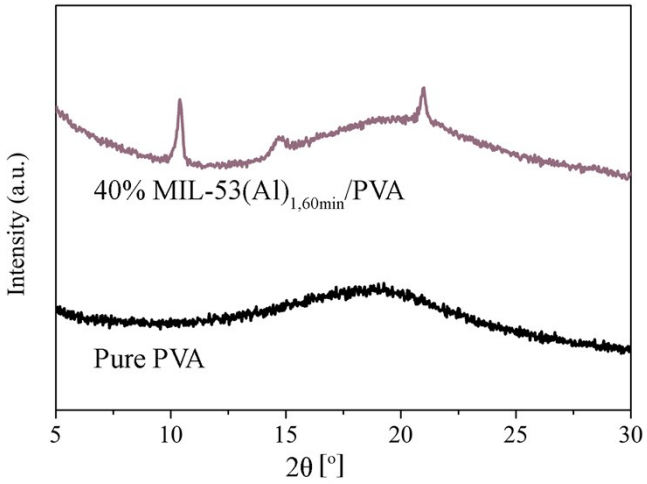

Figure S29. XRD patterns of the MIL-53(Al)/PVA films.

S12 FIB-SEM analysis of the MIL-53(Al)/PVA films

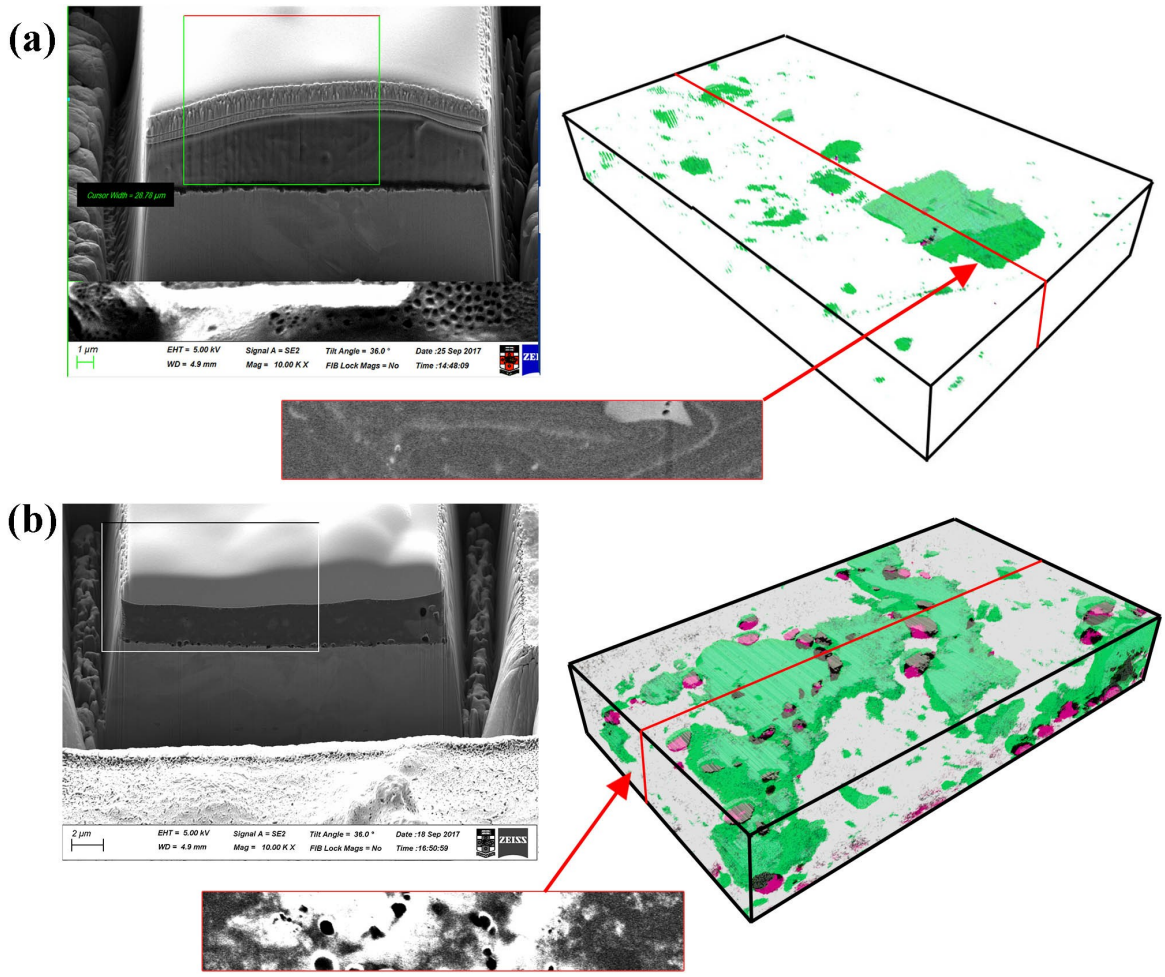

Figure S30. Tomographic FIB-SEM analysis of (a) MIL-53(Al)$_{1,15min}$/PVA and (b) MIL-53(Al)$_{1,60min}$/PVA films. MOF particles are shown in green, while voids are shown in purple. The dimensions of the boxes are 9.25, 1.5 and 5.0 µm, respectively. The insert are reference SEM images for the highlighted cross-sectional area.

S13 Membrane pervaporation test with single brine solution and membrane cleaning

S13.1 Membrane pervaporation experimental setup

The submerged pervaporation setup is shown in Scheme S1. The composite hollow fiber membrane was soaked in the feed solution, which was heated in the water bath with the temperature maintained at 80°C, unless otherwise stated. The permeate water vapour was withdrawn by the peristaltic pump on the permeate side with vacuum pressure around -95 kPa, and collected in the beaker on the balance after condensing. During the operation, the feed tank was topped up every 24 hours using the same solutions at the original feed concentration.

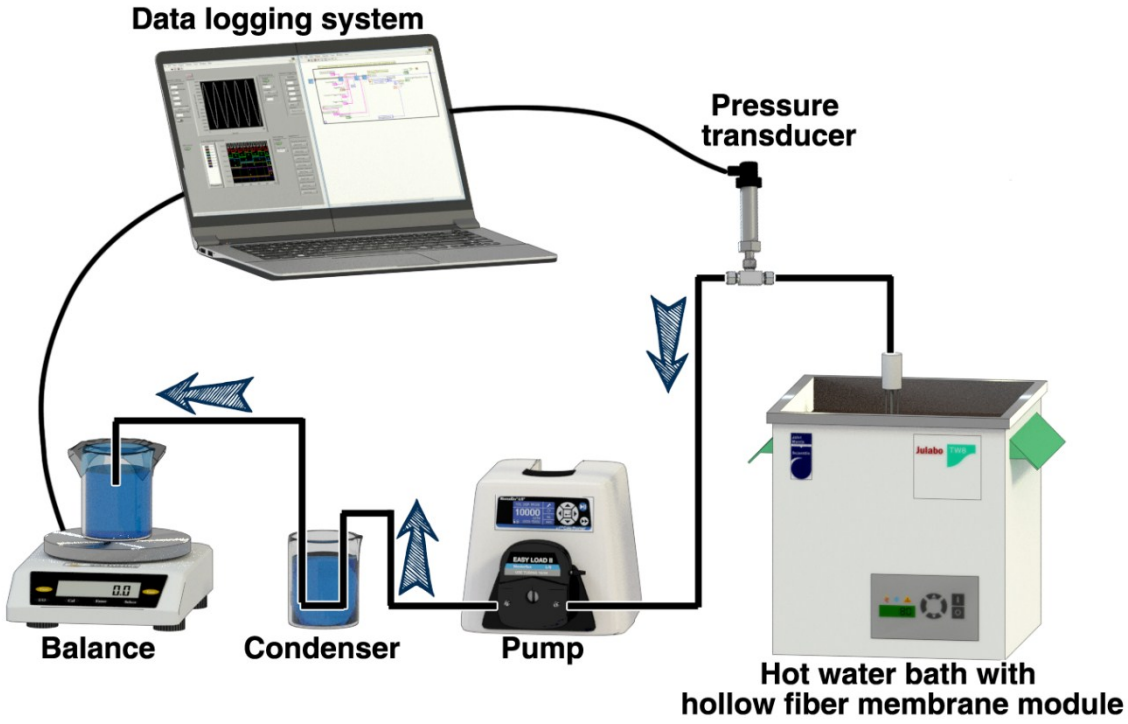

Scheme S1. Schematic diagram of the submerged pervaporation setup with hollow fiber membrane module.

The permeate flux and salt rejection were used to evaluate the pervaporation desalination performances of the composite membranes. The salt rejection (R) was calculated by the following equation, assuming that the conductivity is under linear relationship with concentration.

$$R = \frac{C_f - C_p}{C_f} \times 100\% = \frac{k_f - k_p}{k_f} \times 100\% \qquad \text{(Equation S2)}$$

Where C_f and C_p referred to the feed and permeate salt concentration, κ_f and κ_p referred to the feed and permeate conductivity.

S13.2 Single brine and fouling test

For the single salt brine test, 100 g/L NaCl solution was used as the feed. To explore the membrane's anti-fouling property, certain amounts model foulant including humic acid and calcium chloride were added to the highly concentrated sodium chloride feed solution. Inductively coupled plasma (ICP, PerkinElmer NexION 300) was used to analyze the permeate solutions for inorganic experiments to determine trace concentrations of inorganic elements.

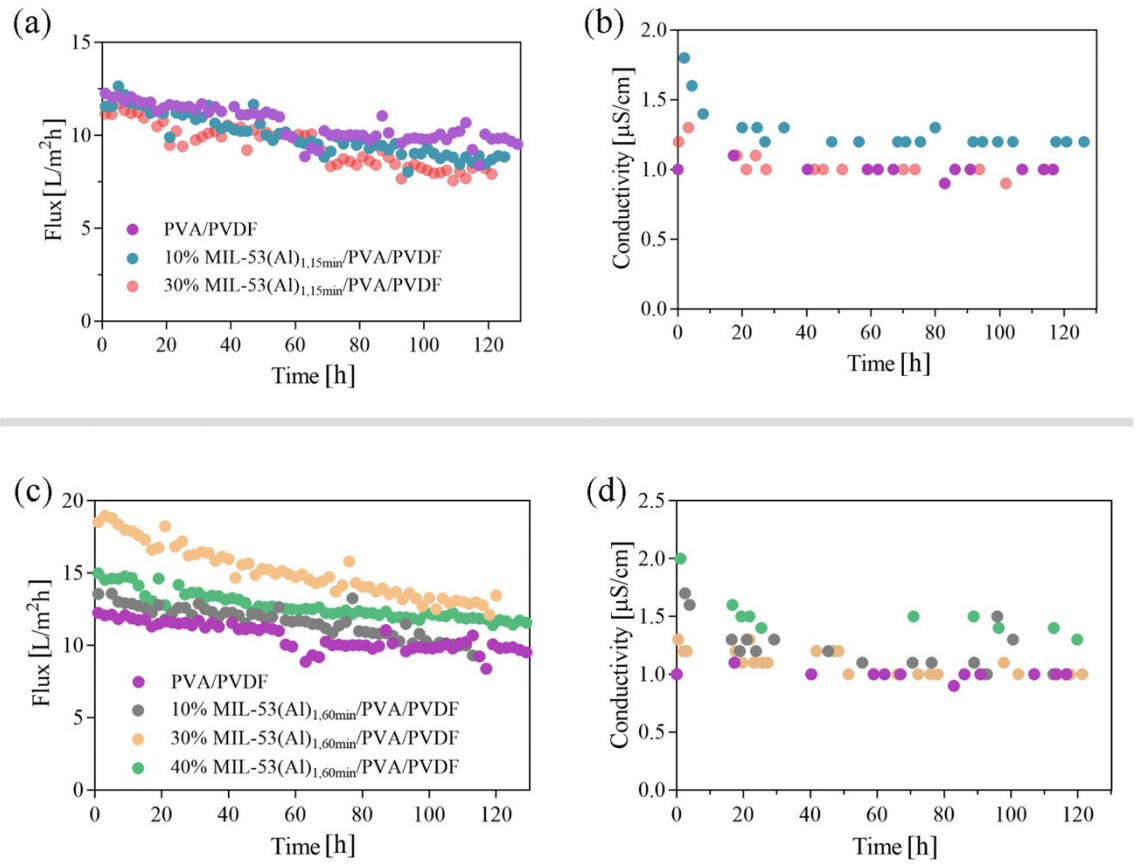

Figure S31. Pervaporation desalination with the nanocomposite membranes containing different MIL-53(Al) MOFs. Feed solution was 100 g/L NaCl at 80 ºC.

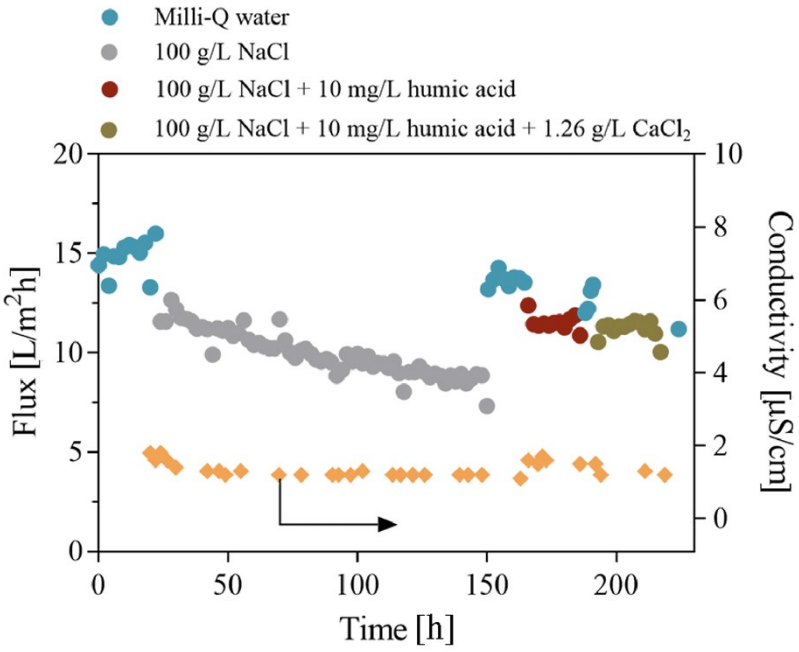

Figure S32. Long term desalination performance with the complex brine feeds at 80 °C and 30 % MIL-53(Al)$_{1,15min}$/PVA/PVDF membrane.

S13.3 Model inland desalination brine test

Model inland desalination brine solution, containing Na^+, Mg^{2+}, Ca^{2+}, Cl^-, SO_4^{2-}, and HCO_3^-, was used as feed solution to evaluate the composite PVA-MIL-53(Al)/PVDF membrane's performance. The detailed components of the brine are listed below:

Table S4. Component of the model inland desalination brine solution.

Salt	Concentration (g/L)
Sodium Chloride (NaCl)	5.84
Magnesium Chloride hexahydrate ($MgCl.6H_2O$)	3.25
Calcium Chloride ($CaCl_2$)	0.35
Sodium Sulphate (Na_2SO_4)	0.76
Sodium Hydrocarbonate ($NaHCO_3$)	0.73

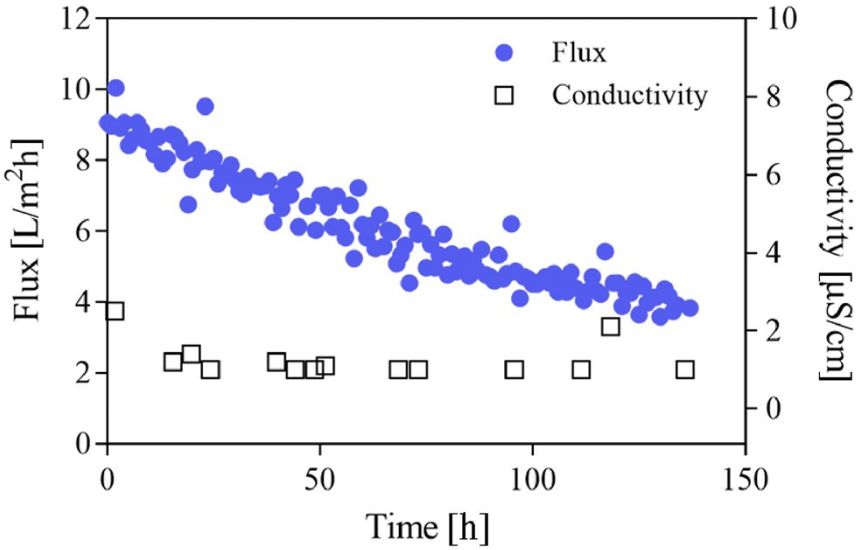

Figure S33. Pervaporation results with the model inland brine solution at 80 °C and 30 % MIL-53(Al)$_{1,15min}$/PVA/PVDF membrane.

Table S5. ICP-MS analysis for the inland brine pervaporation permeate liquid.

Ions	Ca	Mg	Na
Concentration (mg/L)	0.008	0.004	0.103

Table S6. Pervaporation desalination performance for different membranes.

Membrane materials	Membrane configuration[a]	Feed concentration (NaCl, g/L)	Feed temperature (°C)	Selective layer thickness (μm)	Flux (L/m^2h)	Rejection (%)	Ref.
Zeolite in PVA	FS	35	30	/	2.36	96.1	[4]
Silica nanoparticles in PVA	FS	35	65	20	8	99.9	[5]
Silica nanoparticles in PVA	FS	2	22	5	6.93	99.5	[6]
ZIFs on poly-dopamine modified α-Al_2O_3 disks	FS	30	50	20	8.1	99.8	[7]
Electrospraying PVA/electrospinning polyacrylonitrile (PAN)/nonwoven polyethylene terephthalate (PET)	FS	50	Room temperature	0.7	5.57	99.5	[8]
Graphene oxide (GO) sheets on PDA modified Al_2O_3	FS	35	90	0.4	48.4	99.7	[9]
GO on PAN	FS	35	90	0.1	65.1	99.8	[10]
GO with PVA crosslinked by glutaraldehyde on PAN	FS	35	70	0.12	69.1	99.9	[11]
PVA on polysulfone	HF	30	70	0.1	7.4	99.9	[12]
Cross-linked GO by 1,4-phenylene diisocyanate (PDI) on Al_2O_3 substrate	TB	35	90	18	11.4	99.9	[13]
Carbon molecular sieve/polyethylenimine (PEI) on alumina	TB	35	75	/	25	93-99	[14]
MIL-53(Al) in PVA on PVDF	HF	100	80	0.8	18.8	over 99.999 %	This work

[a]FS: flat sheet membrane, HF: hollow fiber membrane and TB: Tubular membrane

S14 References

[1] S. Brunauer, P. H. Emmett, E. Teller, J. Am. Chem. Soc. 1938, 60, 309.
[2] W. Liang, R. Babarao, T. L. Church, D. M. D'Alessandro, Chem. Commun. 2015, 51, 11286; W. Liang, H. Chevreau, F. Ragon, P. D. Southon, V. K. Peterson, D. M. D'Alessandro, CrystEngComm 2014, 16, 6530.
[3] E. P. Barrett, L. G. Joyner, P. P. Halenda, J. Am. Chem. Soc. 1951, 73, 373.
[4] F. U. Nigiz, N. D. Hilmioglu, Desalination and Water Treatment 2014, 1.
[5] Z. Xie, D. Ng, M. Hoang, T. Duong, S. Gray, Desalination 2011, 273, 220.
[6] Z. Xie, M. Hoang, T. Duong, D. Ng, B. Dao, S. Gray, J. Membr. Sci. 2011, 383, 96.
[7] Y. Zhu, K. M. Gupta, Q. Liu, J. Jiang, J. Caro, A. Huang, Desalination 2016, 385, 75.
[8] B. Liang, K. Pan, L. Li, E. P. Giannelis, B. Cao, Desalination 2014, 347, 199.
[9] K. Xu, B. Feng, C. Zhou, A. Huang, Chem. Eng. Sci. 2016, 146, 159.
[10] B. Liang, W. Zhan, G. Qi, Q. Nan, Y. Liu, S. Lin, B. Cao, K. Pan, J. Mater. Chem. A 2015.
[11] C. Cheng, L. Shen, X. Yu, Y. Yang, X. Li, X. Wang, J. Mater. Chem. A 2017.
[12] S. G. Chaudhri, B. H. Rajai, P. S. Singh, Desalination 2015, 367, 272.
[13] B. Feng, K. Xu, A. Huang, Desalination 2016, 394, 123.
[14] Y. Song, D. K. Wang, G. Birkett, W. Martens, M. C. Duke, S. Smart, J. C. Diniz da Costa, Sci. Rep. 2016, 6, 30703.